JCTC Journal of Chemical Theory and Computation

Normal-Mode Analysis of Circular DNA at the Base-Pair Level. 2. Large-Scale Configurational Transformation of a Naturally Curved Molecule

Atsushi Matsumoto,[†,‡] Irwin Tobias,[†] and Wilma K. Olson*[,†]

Department of Chemistry and Chemical Biology, Rutgers, The State University of New Jersey, Wright-Rieman Laboratories, 610 Taylor Road, Piscataway, New Jersey 08854-8087, and Quantum Bioinformatics Group, Center for Promotion of Computational Science and Engineering, Japan Atomic Energy Research Institute, 8-1 Umemidai, Kizu, Kyoto 619-0215, Japan

Received August 31, 2004

Abstract: Fine structural and energetic details embedded in the DNA base sequence, such as intrinsic curvature, are important to the packaging and processing of the genetic material. Here we investigate the internal dynamics of a 200 bp closed circular molecule with natural curvature using a newly developed normal-mode treatment of DNA in terms of neighboring base-pair "step" parameters. The intrinsic curvature of the DNA is described by a 10 bp repeating pattern of bending distortions at successive base-pair steps. We vary the degree of intrinsic curvature and the superhelical stress on the molecule and consider the normal-mode fluctuations of both the circle and the stable figure-8 configuration under conditions where the energies of the two states are similar. To extract the properties due solely to curvature, we ignore other important features of the double helix, such as the extensibility of the chain, the anisotropy of local bending, and the coupling of step parameters. We compare the computed normal modes of the curved DNA model with the corresponding dynamical features of a covalently closed duplex of the same chain length constructed from naturally straight DNA and with the theoretically predicted dynamical properties of a naturally circular, inextensible elastic rod, i.e., an O-ring. The cyclic molecules with intrinsic curvature are found to be more deformable under superhelical stress than rings formed from naturally straight DNA. As superhelical stress is accumulated in the DNA, the frequency, i.e., energy, of the dominant bending mode decreases in value, and if the imposed stress is sufficiently large, a global configurational rearrangement of the circle to the figure-8 form takes place. We combine energy minimization with normal-mode calculations of the two states to decipher the configurational pathway between the two states. We also describe and make use of a general analytical treatment of the thermal fluctuations of an elastic rod to characterize the motions of the minicircle as a whole from knowledge of the full set of normal modes. The remarkable agreement between computed and theoretically predicted values of the average deviation and dispersion of the writhe of the circular configuration adds to the reliability in the computational approach. Application of the new formalism to the computed modes of the figure-8 provides insights into macromolecular motions which are beyond the scope of current theoretical treatments.

Introduction

Although the average properties of polymeric DNA resemble those of an ideal elastic rod, the fine structure of the double helix carries a sequence-dependent structural and energetic code which helps to organize the overall folding of the long, threadlike molecule, and which also governs the susceptibility of DNA to interactions with other molecules. Individual base-pair steps adopt characteristic spatial forms and show different deformational tendencies in high-resolution structures.[1] These local turns and twists, if appropriately concat-

* Corresponding author phone: (732)445-3993; fax: (732)445-5958; e-mail: olson@rutchem.rutgers.edu.

[†] Rutgers, The State University of New Jersey.

[‡] Japan Atomic Energy Research Institute.

10.1021/ct049949s CCC: $30.25
Published on Web 12/21/2004

enated and then repeated in phase with the (~10 bp/turn) double helical repeat, introduce a natural "static" curvature or superhelicity in the DNA,[2−4] which in turn guides the spatial arrangements of longer molecules.[5−7]

Calculations that account for the natural curvature of DNA indicate that polymers with such features adopt completely different three-dimensional arrangements from an ideal, naturally straight elastic rod. For example, a naturally closed circular duplex is expected to take up ligand-induced superhelical stress through out-of-plane folding, gradually converting at natural levels of supercoiling into a 2-fold symmetric collapsed (clamshell-like) figure-8 configuration,[8−15] whereas a closed ideal rod retains a circular shape and snaps suddenly into a plectonemic structure at a characteristic level of supercoiling.[16−18]

The effect of curvature on the dynamical features of DNA, such as the retarded movement of naturally curved sequences on electrophoretic gels, is less well understood. Most modeling studies of the dynamics of naturally curved helices have focused to date on the variation of chemical fine structure extracted from all-atom simulations of the motions of short oligonucleotide duplexes.[19−24] Other work has addressed the bending, spinning, and tumbling of the molecule as a whole in the context of the physical manipulation of naturally curved elastic rods,[25] time-resolved electron microscopic images of single naturally curved molecules,[26] and selected spectroscopic properties of DNA chains containing curved fragments, e.g., electric dichroism decay and fluorescence depolarization of intercalated ethidium dyes in short, naturally curved sequences.[27,28]

Much less is known about the internal dynamics of supercoiled molecules with intrinsic curvature. The insertion of curved sequences in a naturally straight DNA is reported to reduce the internal motions that underlie the dynamic light scattering of supercoiled plasmids.[29] That is, the global configuration of the closed circular molecule is stiffened in the presence of curved DNA such that the likelihood of close approach between interacting fragments is increased and the slithering of individual residues past one another is decreased.[30] By contrast, sufficient increase in the intrinsic curvature of a closed circular molecule introduces a bimodality in the distribution of Monte Carlo simulated configurations of DNA.[31]

In this paper, as a next step in understanding the behavior of curved DNA, we investigate the internal dynamics of a covalently closed, naturally circular double helix. We compare the computed normal modes of such a molecule with the corresponding dynamical features of a cyclized duplex of the same chain length constructed from naturally straight DNA and with the theoretically predicted dynamical properties of a naturally circular, inextensible elastic rod. We present and make use of a general analytical treatment of the configurational fluctuations of an elastic rod. We examine mesoscopic pieces of DNA, fragments too long to investigate at the all-atom level and too complex to approximate as hinged objects, e.g., rigid rods connected by flexible joints. We vary the degree of intrinsic curvature and the superhelical stress on the DNA and consider the normal-mode fluctuations of both the circle and the stable figure-8 configuration under conditions where the energies of the two states are comparable. In this way we are able to decipher the low frequency modes and the enhancement in overall flexibility that underlie the large-scale rearrangement of the naturally curved molecule between the two configurations and gain new insight into the circle to figure-8 transition of supercoiled DNA.

Methods

Computational Treatment. We consider a chain which forms a closed minicircle in its equilibrium rest state. The rest state is defined by the base-pair step parameters identified in the companion paper[32] for the energy-minimized circular form of a DNA molecule which is naturally straight at equilibrium. The natural minicircle is thus described by a 10 bp repeating pattern of intrinsic local structure, with the bending components at each base-pair step, (θ_1^u, θ_2^u), equated to the values of Tilt° and Roll° along the contour of the minimized circular configuration. Values of Tilt and Roll used as references in the calculation of energy, i.e., θ_1^u and θ_2^u in eq *I*-1, where the *I* refers to the companion paper,[32] thus depend on chain length and imposed intrinsic Twist (see Table *I*-2). The treatment is applicable to lengths of DNA such that, when the molecule is constrained to be planar, the total twist of the ideal minicircle, $Tw = \Sigma\, \theta_3^\circ/360°$, is an integer. Here this constraint is satisfied by choosing θ_3° for the planar molecule to be 36° at all base-pair steps and n_B, the number of base-pair steps, to be 200. The normalized sum, which is equal to 20 is the linking number *Lk* of the closed ring, i.e., the number of times the two strands of the double helix wrap around one another. Values of the intrinsic Twist θ_3^u are assumed, however, to be independent of sequence and are assigned a range of values consistent with known environmentally induced changes, e.g., the dependence on temperature or ionic strength.[33−35] If there are no spatial constraints on the ends of the chain, the variation of θ_3^u to a value different from θ_3° converts the circular equilibrium structure to a helical configuration.[36−39] If the chain ends are covalently linked, the total increase or decrease of intrinsic Twist relative to the unligated structure, $\Delta Tw° = (\theta_3^\circ - \theta_3^u)n_B/360°$, imposes torsional stress on the naturally circular molecule. The excess twist in the closed circular configuration, $\Delta Tw°$, is equal to $-\tau^u L/2\pi$, where τ^u is the torsion of the helical pathway of the unlinked chain with intrinsic Twist θ_3^u and *L* is the length of the helical axis.[39−41] (The quantity $\Delta Tw°$, frequently called the linking number difference ΔLk, is the sum of the excess twist ΔTw and the writhing number *Wr*, or writhe for short, of any other configuration.) The molecule is assumed to be inextensible with the displacement of base pairs assigned values characteristic of B DNA, namely zero values of Slide and Shift and a Rise of 3.4 Å. The contour length *L* is therefore equal to 3.4 n_B Å.

The natural minicircle is subject to the same simplified elastic potential as the ideal, naturally straight, inextensible DNA molecule treated in the companion paper.[32] That is, the molecule bends isotropically at all base-pair steps, and the deformations of individual base-pair step parameters are independent of one another. Even though the equilibrium

structure of the DNA is a closed circle, restraints must be introduced in the normal-mode analysis to ensure that the chain termini are connected in the nonequilibrium states. Otherwise, the two ends of the double helix would fly apart as the chain undergoes conformational fluctuations. Thus, a restraint energy term like eq *I*-2 is included in the potential energy function, and an energy minimization step is carried out prior to normal-mode calculations.

Analytical Treatment. It was pointed out in paper *I*, in a discussion of some of the results of an analytical treatment of the normal modes of a circular DNA formed from a naturally straight elastic rod, that the normal-mode frequencies can be obtained by finding the roots of a polynomial cubic in the square of the frequencies. The same turns out to be the case for circular rings formed from intrinsically curved rods.[39] In this paper we compare the frequencies of some of the computed low-order modes of a naturally closed DNA minicircle with those determined from the analytical theory.

The ensemble average of various properties of a collection of identical elastic rods in thermal equilibrium at a temperature T can be extracted from the configuration integral

$$Z = \int e^{-E_\eta/k_B T}\, d\eta \tag{1}$$

an integral of $\exp[-E_\eta/k_B T]$ over all configurations, where E_η is the elastic energy of the rod in a configuration denoted by η and k_B is the Boltzmann constant. Since for the small rings we treat here, the only configurations which make a significant contribution to Z are those close to the equilibrium configuration, we first rewrite eq 1 in the form

$$Z = e^{-E^e/k_B T} z \tag{2}$$

where

$$z = \int e^{-(E_\eta - E^e)/k_B T} d\eta \tag{3}$$

and E^e is the elastic energy of the equilibrium configuration. To obtain information about the distribution of the writhe Wr for the ring-like molecules being considered here, it turns out, as we show below, that what is needed is the explicit dependence of $E_\eta - E^e$ on the topological invariant, the excess twist $\Delta Tw°$ characterizing the circular equilibrium configurations. Only the elastic twist energy contains a term that explicitly involves $\Delta Tw°$, namely, $(2\pi^2 C/L)(\Delta Tw° - Wr)^2$, where C is the twisting modulus. Therefore there is only one term in $E_\eta - E^e$ which contains $\Delta Tw°$ explicitly, $-(4\pi^2 C/L)\Delta Tw° \Delta Wr$, where ΔWr is the writhe associated with a configuration relative to that in the equilibrium configuration. Given the form of this expression, if the integration in eq 3 is now carried out over all configurations of a given writhe, z is of the form

$$z = \int_{-\infty}^{+\infty} e^{[4\pi^2 C/Lk_B T]\Delta Tw° \Delta Wr} F(Wr)\, dWr \tag{4}$$

where $F(Wr)$ is a function of the writhe alone.

The integrand in eq 4 represents the distribution function for the writhe. We see that $\langle \Delta Wr \rangle$, the ensemble average of the writhe relative to that in the equilibrium configuration is given by

$$\langle \Delta Wr \rangle = \left(\frac{Lk_B T}{4\pi^2 C}\right) \frac{\partial \ln z}{\partial \Delta Tw°} \tag{5}$$

The variance of the writhe, $\langle Wr^2 \rangle - \langle Wr \rangle^2$, is obtained by differentiating ln z again, or, given eq 5, it can be written

$$\langle Wr^2 \rangle - \langle Wr \rangle^2 = \left(\frac{Lk_B T}{4\pi^2 C}\right) \frac{\partial \langle \Delta Wr \rangle}{\partial \Delta Tw°} \tag{6}$$

For small elastic rings, the configuration integral is proportional to the high-temperature form of the partition function for a collection of harmonic oscillators having the frequencies $\omega_i(\Delta Tw°)$ of the normal modes of the elastic ring. That is, $z(\Delta Tw°)$ is proportional to the product

$$\prod_i \frac{k_B T}{\hbar \omega_i(\Delta Tw°)}$$

where $\hbar$ is Planck's constant divided by 2π. Knowing the dependence of the normal-mode frequencies on $\Delta Tw°$ is therefore sufficient for determining the average writhe and the variance of the writhe.

In a later section we also compare the average writhe, as given by eq 5, and the variance of the writhe, as given by eq 6, for the two approaches, the computational treatment and the analytical theory.

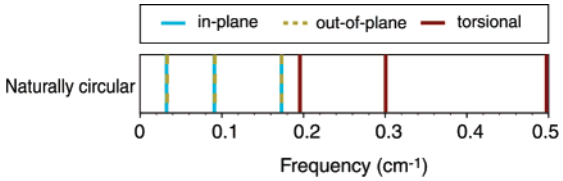

Figure 1. Color coded-spectrum of lowest frequency torsional (unbroken red line), in-plane (unbroken blue line), and out-of-plane (broken green line) modes of a 200 bp torsionally relaxed, inextensible, naturally circular DNA molecule subject to an ideal elastic force field.

Results and Discussion

Natural Minicircle. We start with a 200 bp DNA minicircle with an equilibrium Twist $\theta_3^u = \theta_3^\circ = 36°$, i.e., $Lk = 20$, and local intrinsic bending, given by the variation of Tilt° and Roll° in Table *I*-2, which naturally closes the chain into a circle. As evident from the color-coded spectrum of lowest frequency normal modes in Figure 1, the naturally circular molecule exhibits the same kinds of global motions as a straight chain with covalently linked ends in the torsionally relaxed state, namely in-plane and out-of-plane bending (unbroken blue and broken green lines, respectively) plus large-scale torsional movements of the polymer (red lines) about the circular helical axis. Unlike circles made up of naturally straight DNA, where the ease of in-plane and out-of-plane bending differs, the frequencies of in-plane and out-of-plane deformations of the closed naturally circular molecule are virtually identical. Moreover, these frequencies are roughly equivalent to the frequency of in-plane bending of a cyclized naturally straight chain (Figure *I*-5).

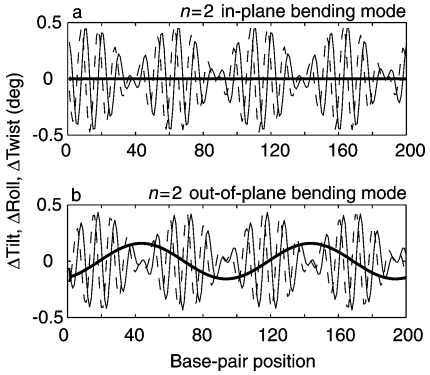

Figure 2. Fluctuations of local angular "step" parameters which are collectively responsible for selected normal modes of a 200 bp torsionally relaxed DNA which forms a natural minicircle in its equilibrium rest state and is subject to an ideal elastic potential: (a) one of the pair of lowest frequency ($n = 2$) in-plane bending modes and (b) one of the pair of lowest frequency ($n = 2$) out-of-plane bending modes. Plots illustrate the fluctuations of Tilt (thin solid lines), Roll (dashed lines), and Twist (thick solid lines) along the contour of the DNA molecule at the moment when the potential energy of the molecule is raised by $k_BT/2$; fluctuations are reversed a half cycle later of the mode.

The difference in the out-of-plane bending modes of naturally circular vs naturally straight DNA arises from a different pattern of local conformational motions. The fluctuations in base-pair step parameters (ΔTilt, ΔRoll, ΔTwist) which give rise to the lowest frequency in-plane and out-of-plane motions of a 200 bp covalently closed, naturally circular molecule, are reported in Figure 2. Comparison of these plots, which capture the local conformational distortions at the instant when the energy of the DNA is raised by $k_BT/2$, with those computed for the straight molecule closed into a circle (Figure *I*-7) reveals a notable difference in the twisting of the intrinsically curved chain. Whereas ΔTwist is close to zero for the out-of-plane deformations of straight DNA, it assumes nonzero values for the corresponding changes in the natural minicircle. By contrast, the patterns of fluctuations associated with the in-plane modes are similar for the two types of circular molecules.

The nonzero ΔTwist in the out-of-plane modes is a natural consequence of intrinsic curvature. Suppose we have a straight piece of DNA with unlinked ends and a planar, curved molecule, e.g., a fragment of naturally circular DNA, with the same contour length and we introduce the same amount of excess Twist at the central base-pair step in the two molecules. The straight DNA retains its original linear global shape, but the curved DNA responds to the imposed deformation through an out-of-plane configurational rearrangement. A DNA which is intrinsically more curved would undergo an even larger out-of-plane movement. The out-of-plane motions of intrinsically curved DNA can thus be effected by changes of Twist as well as by changes of Tilt and Roll, and a more curved piece of DNA can undergo out-of-plane motions more easily. Although the situation is complicated by the constraints of covalent bond formation in cyclic molecules, the involvement of nonzero ΔTwist persists in the out-of-plane modes of naturally circular DNA. Just as a linear molecule of greater curvature undergoes larger out-of-plane movements than a straighter fragment subject to the same amount of added Twist, a circular DNA molecule made up of highly curved pieces is expected to have lower out-of-plane bending frequencies and larger contributions from ΔTwist to the normal modes of bending than a cyclized molecule constructed from naturally straight DNA.

As is clear from comparison of Figures 1 and *I*-5, the torsional frequencies of the intrinsically curved molecule are much higher than those of a cyclized, naturally straight DNA molecule. Whereas the lowest frequency torsional mode of a naturally straight chain closed into a circle is very close to zero, the corresponding frequency of the natural minicircle is much higher. The same conformational mechanism, namely concerted changes in Tilt and Roll, which move base pairs from the inside to the outside of the circle and vice versa, effects global torsional movements in the two molecules. The deformations, however, place a greater conformational energy penalty on the natural minicircle than on cyclized straight DNA. The uniformity of equilibrium Tilt and Roll in the straight chain, $\theta_1^u = \theta_2^u = 0°$, gives rise to a residue-invariant contribution to the bending energy, that allows for all rotational orientations of base pairs and consequent "free rotation" of base pairs about the global helical axis. The corresponding shift of Roll and Tilt in the naturally circular molecule is energetically more costly than that in the straight chain. As a result, the naturally circular DNA has a higher barrier to large-scale helical rotation and higher ($n = 0$) torsional frequencies than a closed, intrinsically straight, ideal rod.

DNA Circles with Variable Intrinsic Curvature. We next consider a series of naturally curved molecules of varying intrinsic curvature κ^u, but all of a length corresponding to 200 bp and all planar ($\tau^u = 0$) in their undeformed open configuration. As discussed previously, when the condition of a uniform double helical repeat of 10 bp per turn is also satisfied, the closed, torsionally relaxed, circular molecule having a curvature $\kappa° = 2\pi/200\Delta s$, where (base-pair displacement) $\Delta s = 3.4$ Å, is in a minimum energy configuration. We report in Figure 3 the dependence of the frequencies of various kinds of global deformations on the value $q = \kappa^u/\kappa°$ for a series of such 200 bp DNA minicircles. (For a given value of the ratio *C*/*A* of the torsional and bending constants, there is a value of q, above which the circle is no longer stable.[39] In the present case, this occurs for a value of q somewhat greater than 2.) Note that, although the values of Tilt, Roll, and Twist of the minimum energy configurations of the minicircles are independent of q, the amplitudes of Roll and Tilt differ from that in the open undeformed configurations (see Table *I*-2) by an amount $(1 - q)\ 360°/200$. We can thus state that the elastic bending energy of the minicircles is proportional to $(1 - q)^2$. The ratio q can also be expressed in terms of the contour length $\tilde{L}$, measured in base pairs, for which the open molecule would form a complete circle, namely, $q = 200/\tilde{L}$.

The variation of the computed lowest frequency ($n = 0$) torsional mode in Figure 3(a) shows remarkable agreement with the theoretically predicted dependence on q.[41] The

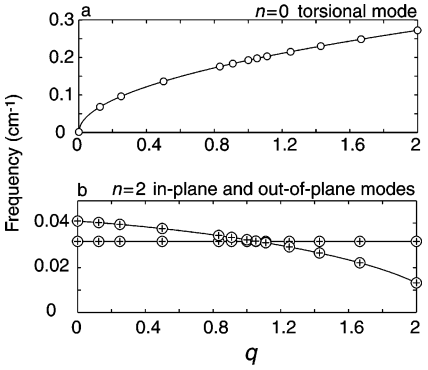

Figure 3. Normal-mode frequencies for (a) the $n = 0$ torsional and (b) the $n = 2$ in-plane and out-of-plane bending modes of naturally curved molecules which are closed into a chain of 200 bp. Data are reported as a function of the ratio $q = \kappa^u/\kappa^\circ$ of the intrinsic curvature κ^u to the curvature κ° of the minimum energy configuration of the natural minicircle. Computed values of the torsional mode frequencies (denoted by o) are compared with the theoretically predicted frequencies (shown by the smooth curve). The degeneracy of the in-plane and out-of-plane modes is evident from the computed frequencies, which are distinguished by o and + symbols and overlaid on the corresponding theoretically predicted curves.

numerical data (open circles) closely match the expected proportionality to $q^{1/2}$ (smooth curve). As observed in paper *I*, the lowest torsional frequency of a circle made from a naturally straight rod is zero. Here we see that this behavior follows from the null value of q. Moreover, the computed magnitude of the lowest torsional frequency of the naturally curved molecules is identical to the theoretically predicted value, e.g., a computed and predicted frequency of 0.19253 cm^{-1} for the natural $q = 1$ minicircle.

There is similar correspondence in Figure 3(b) between the computed and theoretically predicted frequencies of the lowest ($n = 2$) in-plane and out-of-plane bending modes of circular molecules with different degrees of intrinsic curvature. As noted above, the frequency of the out-of-plane bending mode is higher than that of the in-plane mode if the molecule is naturally straight ($q = 0$) but is of comparable magnitude if the DNA forms a natural minicircle ($q = 1$). The two modes are predicted by the theory to be identical in the present case when $q = 1.06$ and found by the calculations to be equivalent at approximately the same value. (An exact comparison is precluded by the limitations on chain length in the calculations, i.e., multiples of 10 bp.[32]) The ease of out-of-plane bending becomes greater than that of in-plane deformation, i.e., of lower frequency and lower energy, if q exceeds this threshold. That is, molecules which are more strongly bent, i.e., chains which cyclize into smaller rings than the natural minicircle, show a natural tendency to fluctuate out of the plane of the 200 bp circle. Indeed, when $q = 2$ and $C/A = 1$ and the molecule is closed into a circle two times the length of its equilibrium rest state, the barrier to out-of-plane deformations is removed, and the frequency of the mode is close to zero.[39,42] By contrast, the frequencies of the in-plane modes of the torsionally relaxed minicircle are predicted and found through computation to be constant over this range of q.

The difference in Twist fluctuations noted above for circles of naturally straight and naturally circular DNA also depends on the value of q. That is, when q is small, the amplitude of ΔTwist in the out-of-plane bending modes is small compared to that of either ΔTilt or ΔRoll, but as q increases in value, the amplitude of ΔTwist becomes comparable to the amplitudes of the local bending parameters (data not shown).

Properties of Supercoiled Molecules. *Figure-8 Minimum.* As with naturally straight DNA, superhelical stress can be introduced into the natural minicircle by changing the intrinsic Twist. If the change is sufficiently large, a global configurational rearrangement takes place, with the DNA adopting a figure-8 rather than a circular minimum energy state. This transition also occurs in closed molecules made up of naturally straight DNA,[17,18] but since there are no self-contact terms[43] in the present calculations, the figure-8 configuration of a naturally straight DNA is unstable and not found upon energy minimization. In the case of naturally circular DNA, energy minimization identifies a figure-8 minimum energy structure, which makes it possible to monitor details of the large-scale (circle to figure-8) spatial rearrangement.

Here we again study a 200 bp natural DNA minicircle subject to the same ideal elastic force field employed above, i.e., $A = 2.1 \times 10^{-19}$ erg-cm, $C = 2.9 \times 10^{-19}$ erg-cm. The equilibrium values of the base-pair step parameters are taken from the expressions for Tilt° and Roll° in Table *I*-2 or eq *I*-6, which close a naturally straight molecule of specified length and equilibrium Twist, θ_3°, into a circle. The transition to the figure-8 occurs when the intrinsic Twist θ_3^u differs by about $\pm 1.8°$ from θ_3°, changes which are equivalent to the introduction of $\pm 360°$ of additional twist into the DNA. By contrast, 1.25 additional helical turns are required to effect the interchange of stability between a closed circle and the figure-8 configuration of naturally straight DNA under the same elastic potential, i.e., a critical twist increment of $\pm\sqrt{3}\ A/C$ helical turns.[16−18] Figure 4 shows the minimum energy figure-8 structure obtained when the intrinsic Twist of the minicircle differs from θ_3° by $\pm 1.8°$, i.e., $\theta_3^u = 34.2°, 37.8°$. As is clear from the color coding in the figure, the Twist of individual base-pair steps is nonuniformly distributed along the two configurations. The uptake of Twist is concentrated in the center of the structures. The twisting of successive base pairs remains close to the 36° value characteristic of torsionally relaxed DNA in the 180° turns at the two (hairpin) ends of each structure. The slight difference in the respective writhes of the two figure-8's, +1.05 and −1.05, from the values (± 1) characteristic of the ideal planar forms reflect the finite radius of the DNA model (~10 Å). Details of the best-fit cosine functions, which describe the variation of base-pair step parameters along the minimum energy structures, are summarized in Table 1. The two dominant terms are presented. Comparison of these functions with those fitted to the minimum energy circular state adopted by the same chain (Table *I*-2) reveals an additional cosine term of wavelength of 11.1 bp or 9.1 bp, numbers corresponding respectively to 10/9 or 10/11 of the 10-fold helical repeat of the relaxed equilibrium state.

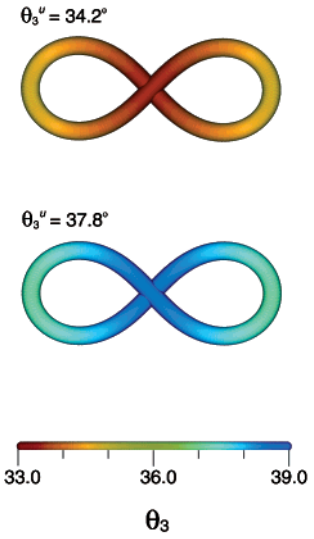

Figure 4. Computer-generated representation[52] of the minimum energy figure-8 configurations of a natural 200 bp DNA minicircle obtained by changing the intrinsic Twist θ_3^u by $\pm 1.8°$ from the equilibrium value θ_3^o in the torsionally relaxed state. The color coding depicts the value of Twist θ_3, in degrees, at consecutive base-pair steps along the two equilibrium structures.

Table 1. Base-Pair Step Parameters at the *m*th Dimer Step of an Ideal, Inextensible[a] Supercoiled DNA Circle of 200 bp in the Figure-8 Minimum Energy State

description	sequential conformational state
$\theta_3^u = 34.2°$ (figure-8 form)	
	Tilt° = 1.857 cos((360/11.1)(m + 0.553)) + 2.468 cos(36(m − 0.500))
	Roll° = 1.857 cos((360/11.1)(m + 0.553) + 90) + 2.468 cos(36(m − 0.500) + 90)
	Twist° = 34.108 + 0.671 cos((360/100)(m − 9.979))
$\theta_3^u = 34.25°$ (figure-8 form)	
	Tilt° = 1.864 cos((360/11.1)(m + 0.508)) + 2.460 cos(36(m − 0.500))
	Roll° = 1.864 cos((360/11.1)(m + 0.508) + 90) + 2.460 cos(36(m − 0.500) + 90)
	Twist° = 34.308 + 0.663 cos((360/100)(m − 9.571))
$\theta_3^u = 37.8°$ (figure-8 form)	
	Tilt° = 2.468 cos(36(m − 0.500)) + 1.857 cos((360/9.1)(m − 1.042))
	Roll° = 2.468 cos(36(m − 0.500) + 90) + 1.857 cos((360/9.1)(m − 1.042) + 90)
	Twist° = 37.891 − 0.670 cos((360/100)(m − 6.460))

[a] (Shift°, Slide°, Rise°) = (0 Å, 0 Å, 3.4 Å).

Bending Modes of the Torsionally Stressed Minicircle. Figure 5 reports the lowest bending frequencies of the natural minicircle as a function of intrinsic Twist θ_3^u. This figure is a counterpart to Figure *I*-11(a), obtained for a naturally straight elastic chain closed into a circle of the same length (200 bp). Here the range of imposed stress is extended beyond that presented in paper *I*. The computed bending modes are represented by discrete points and the predictions of theory by smooth curves. The superposition of symbols—open circles and plus signs for the natural minicircle, open boxes and cross symbols for the over- or undertwisted circle

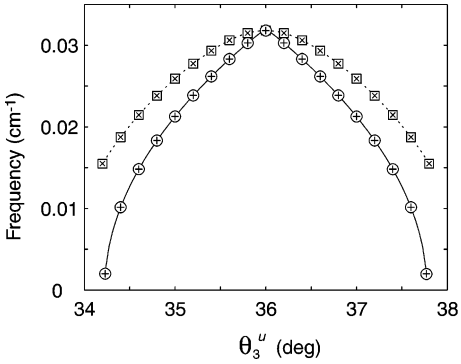

Figure 5. Lowest normal-mode frequencies of bending of a 200 bp natural DNA minicircle subject to an ideal elastic force field and the corresponding cyclic polymer made up of naturally straight DNA as a function of the intrinsic Twist θ_3^u. The degenerate frequencies obtained through computations are distinguished by symbols (o and + for the natural minicircle; open box and cross × for the closed, naturally straight DNA). The theoretically predicted values are represented by smooth curves (unbroken for the natural minicircle and broken for the circularized straight DNA).

made up of straight DNA—highlights the degeneracy of the configurational fluctuations, and the nearly perfect fit of these points to the smooth (respectively unbroken and broken) curves illustrates the remarkable agreement of computation and theory. The computed frequencies of the natural minicircle are limited to the range of θ_3^u within which and slightly beyond the limit where the circular form is lower in energy than the figure-8 configuration. The theoretical frequencies are reported for values of θ_3^u up to the point at which the predicted variation in $\langle \Delta Wr \rangle$, the average deviation of the writhe, becomes unphysical.

The primary difference in behavior between the two cyclized polymers lies in the much greater sensitivity of the normal-mode frequencies to changes in the intrinsic Twist in the natural minicircle compared to the cyclized polymer of naturally straight DNA. The decrease in the lowest frequency bending mode in the former chain is more than twice that found for a $\pm 0.5°$ increment of θ_3^u in the latter molecule. Furthermore, the frequency of deformation of the natural minicircle drops precipitously if the intrinsic Twist is changed slightly more, approaching a value of zero if θ_3^u is changed by $\pm 1.8°$, the same critical value associated with the interchange of the naturally circular and figure-8 minimum energy rest states. The very low frequency of these modes indicates that the energetic cost of deforming the over- or undertwisted circle into a different shape is negligible. The bending frequencies of the cyclized naturally straight DNA approach the same low-energy values when θ_3^u differs by $\pm 2.26°$ from the equilibrium state.

The nature of this large-scale configurational rearrangement is evident from the computed fluctuations in Figure 6 of individual base-pair origins with respect to (**n**°, **b**°, **t**°) Serret-Frenet coordinate frames embedded in each base pair of the energy-minimized, circular reference state. The plots show the displacements of individual residues in over- and undertwisted ($\theta_3^u = 34.25°$ and $37.75°$) natural minicircles at the moment when the potential energy of the DNA is

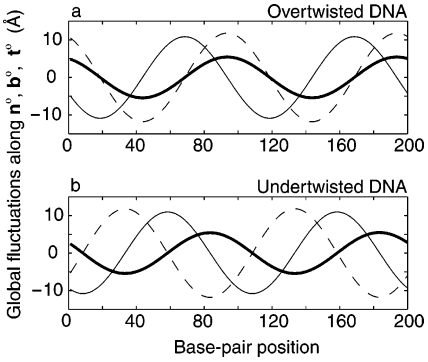

Figure 6. Displacement of the origins of base-pair axes at the moment when the potential energy is raised by $k_BT/50$ in the lowest frequency bending modes of (a) an overtwisted ($\theta_3^u = 34.25°$) or (b) an undertwisted ($\theta_3^u = 37.75°$) 200 bp natural DNA minicircle. Displacements (thin solid, dashed, and thick solid lines) measured respectively along the **n**°, **b**°, **t**° axes of Serret-Frenet frames embedded in each base pair of the minimum energy configuration.

raised by $k_BT/50$ along the lowest frequency mode. The very low-energy threshold in the example is a consequence of the very low frequency of the mode and the restriction of normal-mode analysis to conformational fluctuations in the vicinity of the minimum energy state. (Step parameters lie very far away from the reference state if the mode is assigned a higher energy.) As evident from the displacement along the **b**° axes (normals) of the planar circle (dashed curves), the global motion is no longer a pure in-plane bending mode upon supercoiling. The patterns of macromolecular displacement are quite similar, in terms of relative phase, to the deformations reported in Figure *I*-9 for over- and undertwisted closed circles made up of naturally straight DNA. For example, the largest moves along the **b**° and **t**° axes of the overtwisted natural minicircle in Figure 6(a) occur at the same positions as those of the overtwisted ideal DNA rod in Figure *I*-9(a), and the greatest changes along **n**° again appear 25 bp ahead of these points. The deformations of the natural minicircle, however, are much greater in magnitude than those of the naturally straight molecule under corresponding superhelical stress. The relative contribution of out-of-plane (**b**°-axis) motions also differs in the two molecule, i.e., greater displacements along **b**° and **n**° than along **t**° in the naturally closed molecule but more pronounced motions along **n**° than along either **b**° or **t**° in over- and undertwisted circles composed of naturally straight DNA.

Local Conformational Responses of the Stressed Minicircle. The fluctuations of local step parameters responsible for the lowest frequency mixed bending modes of the over- or undertwisted natural minicircle are summarized by a series of best-fit cosine functions in Table 2. The expressions describe the sequential variation of ΔTilt, ΔRoll, and ΔTwist of one of the degenerate modes for selected values of intrinsic Twist at the instant when the energy is raised by $k_BT/50$. The conformational patterns of the other of the degenerate modes are related by a phase shift of 90° in the fitted cosine functions. In all cases, the sequential variation in dimer bending is described by a sum of cosine functions, one with wavelength 11.1 bp and the other with wavelength 9.1 bp.

Table 2. Fluctuations of Base-Pair Step Parameters at the *m*th Dimer Step of an Ideal, Inextensible,[a] Naturally Circular, Supercoiled DNA Circle of 200 bp in the Lowest Frequency In-Plane Bending Mode

description	sequential conformational distortions
$\theta_3^u = 34.25°$ (overtwisted)	
	$\Delta\text{Tilt} = -0.522\cos((360/11.1)(m + 1.401)) - 0.0215\cos((360/9.1)(m - 2.055))$
	$\Delta\text{Roll} = -0.522\,(\cos((360/11.1)(m + 1.401) + 90) - 0.0215\cos((360/9.1)(m - 2.055) + 90)$
	$\Delta\text{Twist} = -0.179\cos((360/100)(m - 17.610))$
$\theta_3^u = 36°$ (torsionally relaxed)	
	$\Delta\text{Tilt} = -0.0472\cos((360/11.1)(m + 0.193)) - 0.0473\cos((360/9.1)(m + 1.652))$
	$\Delta\text{Roll} = -0.0472\cos((360/11.1)(m + 0.193) + 90) - 0.0473\cos((360/9.1)(m + 1.652) + 90)$
	$\Delta\text{Twist} = 0.000$
$\theta_3^u = 37.75°$ (undertwisted)	
	$\Delta\text{Tilt} = -0.0215\cos((360/11.1)(m + 0.268)) - 0.522\cos((360/9.1)(m - 1.128))$
	$\Delta\text{Roll} = -0.0215\cos((360/11.1)(m + 0.268) + 90) - 0.522\cos((360/9.1)(m - 1.128) + 90)$
	$\Delta\text{Twist} = +0.179\cos((360/100)(m - 7.412))$

[a] (Shift°, Slide°, Rise°) = (0 Å, 0 Å, 3.4 Å).

If the minicircle is torsionally relaxed, the amplitudes of the two terms are roughly equivalent. The function characterized by wavelength 11.1 bp dominates if the intrinsic Twist is decreased to 34.25°, and the function characterized by wavelength 9.1 dominates if the intrinsic Twist is increased to 37.75°. The amplitude of ΔTilt or ΔRoll is fairly large in both cases, increasing by more than 0.5° at some base-pair steps. If Tilt and Roll vary independently of one another, there is, by definition, a 90° phase shift in the terms used to describe the sequential variation of ΔTilt and ΔRoll.

The sequential variation of base-pair step parameters in the minimum energy figure-8 structures of the natural minicircles with intrinsic Twist varied by ±1.8° from the ($\theta_3^\circ = 36°$) equilibrium state (Table 1) bears a remarkable resemblance to the computed fluctuations of local variables in the lowest frequency mixed bending mode of the over- and undertwisted circles (Table 2). As noted above, an additional cosine term of wavelength 11.1 or 9.1 bp appears in the functions fitted to the sequential variation of Tilt and Roll along the optimized figure-8 structures and a term of the same period dominates the bending modes of the natural minicircle with $\theta_3^u = 34.25°$ or 37.75°. Given that no other normal modes of the circle show a comparable decrease in frequency and energy with imposed supercoiling, it is highly likely that these modes guide the transition pathway between the circular and figure-8 forms (see below).

Normal Modes of the Figure-8. Normal-mode analysis of the stable figure-8 minimum of the same ($\theta_3^u = 34.25°$) overtwisted DNA molecule yields a complementary picture of configurational deformation. The lowest (nearly zero) frequency motion of the figure-8 is a slithering motion of the duplex which has no effect on overall macromolecular shape, i.e., the point of chain self-contact simply translocates freely along the molecular contour. The fluctuations of local step parameters responsible for the slithering mode are described by the best-fit cosine functions in Table 3. The expressions, which contain only the dominant contribution

Table 3. Fluctuations of Base-Pair Step Parameters at the *m*th Dimer Step of an Ideal, Inextensible,[a] Naturally Circular, Supercoiled DNA of 200 bp about the Minimum Energy Figure-8 Configuration in the Two Lowest Frequency Bending Modes

description	sequential conformational distortions
$\theta_3^u = 34.25°$ (mode 1, slithering[b])	
	$\Delta\text{Tilt} = 0.185\cos((360/11.1)(m + 0.508) - 90)$
	$\Delta\text{Roll} = 0.185\cos((360/11.1)(m + 0.508))$
	$\Delta\text{Twist} = -0.066\cos((360/100)(m - 9.571) - 90)$
$\theta_3^u = 34.25°$ (mode 2, bending)	
	$\Delta\text{Tilt} = 0.076\cos(36(m - 0.500)) - 0.098\cos((360/9.1)(m - 1.325))$
	$\Delta\text{Roll} = 0.076\cos(36(m - 0.500) + 90) - 0.098\cos((360/9.1)(m - 1.325) + 90)$
	$\Delta\text{Twist} = -0.638 + 0.034\cos((360/100)(m - 9.671))$

[a] (Shift°, Slide°, Rise°) = (0 Å, 0 Å, 3.4 Å). [b] Parametric values when the energy is raised by $k_BT/(2 \times 10^4)$.

for each base-pair step parameter at the moment when the energy is raised by $k_BT/(2 \times 10^4)$, closely resemble the sequential variation of base-pair step parameters along the figure-8 minimum energy state (Table 1). Specifically, the expressions for the fluctuations in Roll and Tilt are obtained by shifting the phase by 90° and reducing the amplitude of the cosine functions with wavelength 11.1 bp. Such variation of parameters is reminiscent of the local conformational changes found in the lowest frequency, "free" torsional mode of a naturally straight DNA closed into a circle, where a corresponding change in phase results in the movement of base-pair steps from the inside to the outer surface of the molecule, and vice versa.[32] In the case of the lowest frequency slithering mode of the figure-8, the local conformational changes move the sites of maximum and minimum bending, located respectively at the two tips and the central crossing points of the figure-8, back and forth along the chain contour. The second lowest frequency motion of the figure-8 is a mixed bending mode which assists in opening the collapsed, self-contacted structure to the circular form (see below). As evident from Table 3, where the fluctuations of local step parameters needed to raise the energy by $k_BT/2$ are reported as fitted trigonometric functions, the residue-invariant increase (or decrease a half cycle later) of ΔTwist dominates this mode.

Thermal Fluctuations. The global motions associated with a collection of thermally fluctuating 200 bp minicircles are illustrated in Figure 7. Equation 5 was used to compute $\langle \Delta Wr \rangle$, the average deviation of the writhe from that in the equilibrium configuration, and eq 6 to compute the square root of the variance of the writhe $(\langle Wr^2 \rangle - \langle Wr \rangle^2)^{1/2}$, both as a function of torsional stress measured by $\Delta Tw° = (\theta_3° - \theta_3^u) \times 200/360°$. The open circles and the ×'s give the results of the computations for naturally curved and intrinsically straight DNA, respectively. In both of these cases, the equilibrium configuration is circular, and the results closely match the predictions of the analytical theory given by the solid and broken curves. In the case of the filled-in circles, the equilibrium configuration is figure-8 like, a case to which the analytical theory has not been applied. The

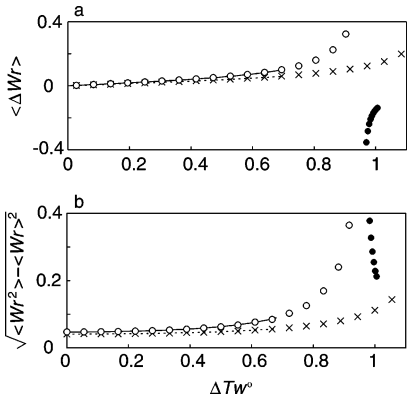

Figure 7. Variation of the average deviation of the writhe $\langle \Delta Wr \rangle$ from that in the circular equilibrium configuration and the square root of the variance of the writhe, $\sqrt{\langle Wr^2 \rangle - \langle Wr \rangle^2}$ vs the total imposed twist, $\Delta Tw°$, of a closed 200 bp naturally circular DNA (open circles), a circular chain of the same length constructed of naturally straight DNA (× symbols), and the figure-8 configuration adopted by the naturally circular molecule (filled-in circles). The theoretically predicted behavior of the two circular configurations is represented respectively by broken and unbroken curves over the range in which the theory is valid.

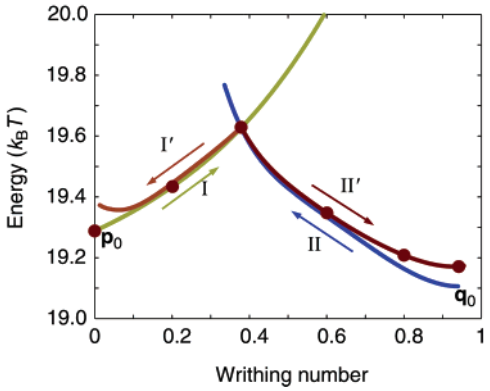

Figure 8. The variation of energy versus writhe of an overtwisted ($\theta_3^u = 34.25°$), naturally circular, 200 bp DNA molecule perturbed along its lowest frequency modes to transient configurational states intermediate between the minimum energy circular and figure-8 forms. The large dots correspond to states illustrated in Figure 10. (See text for details of transition pathways.)

excellent agreement between the present calculations and the analytical theory is evident in the graphs, as is the difference in properties of the rings formed from curved DNA as opposed to straight. The data show the increased flexibility of the natural minicircles as compared with circles formed from intrinsically straight chains for all values of $\Delta Tw°$. The greater sensitivity of the writhe-altering fluctuations of the natural minicircles to increasing torsional stress is also evident.

Pathways of Large-Scale Configurational Rearrangement. *Excursions of the Circle*. Figure 8 reports the variation in both energy and writhe of an overtwisted ($\theta_3^u = 34.25°$), naturally curved DNA minicircle perturbed along its lowest frequency normal modes to transient configurational states intermediate between the (circular and figure-8) minimum

energy configurations found to be stable under these conditions. Path I corresponds to deformations of the circle along the lowest frequency (mixed bending) mode detailed in Table 2 and Path II to the corresponding normal-mode bending distortions of the figure-8 (see below). A writhe of zero corresponds to the circle and a value of unity to an ideal, planar figure-8 configuration. The energy cost of large-scale configurational rearrangements (monitored by the writhe) between the circle and figure-8 is quite small.

The intermediate configurational states in Figure 8 are obtained by recursive introduction of small normal-mode distortions of base-pair step parameters followed by rapid energy minimization. Each configuration of DNA is described by 1200 parameters (6 rigid-body parameters per base-pair step × 200 base-pair steps). The initial (minimum energy) configuration is defined by a 1200 dimensional vector $\mathbf{p}_0$, with elements corresponding to the sequential variation of step parameters around the circle, and is deformed to $\mathbf{p}_0 + \alpha\Delta\mathbf{p}_0$, where α is a constant and the displacement vector $\Delta\mathbf{p}_0$ is the normalized lowest frequency normal-mode vector of the circle. A short run of (conjugate gradient) energy minimization is then carried out to avoid high energy states. The minimization is stopped when the decrease of energy per iteration is small ($<5 \times 10^{-5}\ k_BT$). More thorough energy minimization would return the configuration to the initial state $\mathbf{p}_0$. The constant α is chosen to be small enough so that the number of iterations per minimization cycle is at most 5. The new configuration $\mathbf{p}_1$ is then deformed to $\mathbf{p}_1 + \alpha\Delta\mathbf{p}_1$, where the normalized displacement vector $\Delta\mathbf{p}_1$ is defined by the configurational change from the initial structure, $(\mathbf{p}_1 - \mathbf{p}_0)/|\mathbf{p}_1 - \mathbf{p}_0|$. Energy minimization is performed as in the preceding step, and the new configuration $\mathbf{p}_2$ is obtained. This process is repeated, so that in the kth repetition, configuration $\mathbf{p}_k$ is deformed to $\mathbf{p}_k + \alpha\Delta\mathbf{p}_k$, where $\Delta\mathbf{p}_k$ is defined by the direction of the last configurational move, $(\mathbf{p}_k - \mathbf{p}_{k-1})/|\mathbf{p}_k - \mathbf{p}_{k-1}|$. Energy minimization follows, and the new configuration $\mathbf{p}_{k+1}$ is obtained. In this way, the series of configurations $\mathbf{p}_1 \ldots \mathbf{p}_K$ along Path I is generated, the energy of which is plotted versus the writhe in Figure 8. As should be clear from the above description, the displacement vector $\Delta\mathbf{p}_k$ changes as the configuration of the molecule changes. The correlation of the displacement vectors along Path I with the initial displacement vector $\Delta\mathbf{p}_0$ is reported in Figure 9, Curve *a*. The correlation is greatest at the start of the transformation and decreases approximately linearly with the increase in writhe, i.e., departure from the equilibrium reference state.

Miyashita et al.[44] have recently reported an analogous global transformation of a protein using an elastic network model of amino acid interactions. They use a scheme much like ours to generate intermediate conformational states along the transition pathway between open and closed forms of the molecule. The displacement vector $\Delta\mathbf{p}_k$ ($k > 0$) used to generate successive intermediate states, however, is a combination of the low-frequency normal modes of the current conformation $\mathbf{p}_k$. In contrast to the elastic treatment of DNA, where intermediate conformational states are not minimum energy structures, all molecular states can be regarded as minima in the elastic network model. Thus, we

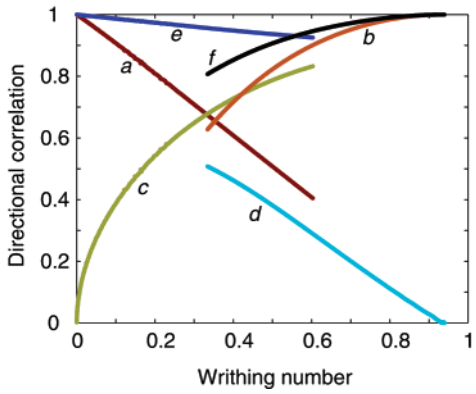

Figure 9. Correlations, plotted against the writhe, of the displacement vectors $\Delta\mathbf{p}_k$ and $\Delta\mathbf{q}_l$ of intermediate configurational states with the normal (bending) mode vectors $\mathbf{p}_0$ and $\mathbf{q}_0$ of the minimum energy circular and figure-8 forms of the overtwisted DNA molecule described in Figure 8: (a) $\Delta\mathbf{p}_k \cdot \Delta\mathbf{p}_0$; (b) $\Delta\mathbf{q}_l \cdot \Delta\mathbf{q}_0$; (c) $-\Delta\mathbf{p}_k \cdot \Delta\mathbf{q}_0$; (d) $-\Delta\mathbf{q}_l \cdot \Delta\mathbf{p}_0$, and the corresponding contributions from the two normal-mode vectors ($\Delta\mathbf{p}_0$ and $\Delta\mathbf{q}_0$) to the displacement vectors ($\Delta\mathbf{p}_k$ and $\Delta\mathbf{q}_l$); (e) $((\Delta\mathbf{p}_k \cdot \Delta\mathbf{p}_0)^2 + (\Delta\mathbf{p}_k \cdot \Delta\mathbf{q}_0)^2)^{1/2}$; (f) $((\Delta\mathbf{q}_l \cdot \Delta\mathbf{p}_0)^2 + (\Delta\mathbf{q}_l \cdot \Delta\mathbf{q}_0)^2)^{1/2}$.

cannot perform normal mode calculations at each stage of conformational transformation and, instead, move from state to state using the aforementioned iterative minimization procedure. The fact that the transition pathway can be described by a small number of normal modes suggests the possibility of identifying a smooth, realistic conformational pathway with a low-energy barrier using more sophisticated approaches, such as path integral techniques.[45]

Excursions of the Figure-8. The second lowest frequency mixed bending mode of the figure-8 is responsible for the large-scale configurational rearrangement needed to open the collapsed, self-contacted structure to the circular form. The series of configurations $\mathbf{q}_1 \ldots \mathbf{q}_L$ along Path II in Figure 8 is generated, starting from the energy-minimized figure-8 configuration $\mathbf{q}_0$ (writhe = 0.94) and the normalized initial displacement vector $\Delta\mathbf{q}_0$ associated with the second lowest frequency bending mode. As with the deformed states of the circle, the correlation of the displacement vector $\Delta\mathbf{q}_l$ with the initial displacement vector $\Delta\mathbf{q}_0$ decreases as the configuration of the molecule changes from its original state, Curve *b* in Figure 9.

Interestingly, the displacement vector $\Delta\mathbf{p}_k$ on Path I describing perturbations of the circle is correlated with the initial displacement vector $\Delta\mathbf{q}_0$ of the figure-8. The correlation $\Delta\mathbf{p}_k \cdot (-\Delta\mathbf{q}_0)$ is plotted as Curve *c* in Figure 9. Initially at the minimum energy (circular) configuration (where $k = 0$), the correlation is close to zero, indicating that the two vectors ($\Delta\mathbf{p}_0$ and $\Delta\mathbf{q}_0$) are almost perpendicular to each other. The correlation increases as the writhe increases. The increase of the correlation complements the decrease of the correlation $\Delta\mathbf{p}_k \cdot \Delta\mathbf{p}_0$ (Curve *a*). Indeed, the contribution from the two directions $((\Delta\mathbf{p}_k \cdot \Delta\mathbf{p}_0)^2 + (\Delta\mathbf{p}_k \cdot \Delta\mathbf{q}_0)^2)^{1/2}$, which is plotted as Curve *e* in Figure 9, is close to unity, indicating that these two normal-mode vectors play dominant roles in the circle to figure-8 transition (Path I). The series of displacement vectors $\Delta\mathbf{q}_l$ along Path II is similarly correlated with $\Delta\mathbf{p}_0$. The correlation $\Delta\mathbf{q}_l \cdot (-\Delta\mathbf{p}_0)$ is plotted

as Curve *d* in Figure 9. In this case also, the contribution from the two directions $((\Delta\mathbf{q}_l \cdot \Delta\mathbf{p}_0)^2 + (\Delta\mathbf{q}_l \cdot \Delta\mathbf{q}_0)^2)^{1/2}$, Curve *f* in Figure 9, is close to unity, indicating that the two normal-mode vectors play dominant roles in the reverse (figure-8 to circle) transformation (Path II).

Intermediate States. Although the writhe is very effectively changed if the DNA is deformed along Paths I and II in Figure 8, the minimum energy configurations of the figure-8 and circular forms ($\mathbf{q}_0$ and $\mathbf{p}_0$, respectively) cannot be reached or approached from the opposing minimum. The direction of the displacement vectors $\Delta\mathbf{p}_n$ and $\Delta\mathbf{q}_m$ must be changed discontinuously at some point to approach the opposite minimum energy states. Paths I′ and II′ in Figure 8 are obtained by such changes. Configurations $\mathbf{p}_{k'}$ and $\mathbf{q}_{l'}$ are the closest points on Paths I and II, respectively, to their point of intersection, differing from one another by a root-mean-square distance of 5.6 Å. Path II′ is obtained by using $\mathbf{p}_{k'}$ as the starting configuration and the $-\Delta\mathbf{q}_{l'}$ as the initial displacement vector. Path I′ is similarly obtained from $\mathbf{q}_{l'}$ and $-\Delta\mathbf{p}_{k'}$. The differences between Paths I and I′ near $Wr = 0$ and those between Paths II and II′ near $Wr = 1$ stem primarily from insufficient energy minimization in the generation of intermediate configurations. The minimum energy configurations $\mathbf{p}_0$ and $\mathbf{q}_0$, where normal-mode calculations are carried out, can be reached only by thorough energy optimization, e.g., Newton−Raphson minimization.

The continuous transformation of the circle to the figure-8 along Paths I and II′ is illustrated in Figure 10 and in the Supporting Information. Starting from the circular configuration, the deformation proceeds primarily via the change of Tilt and Roll (see the expressions in Table 2 for the variation of step parameters in the lowest frequency bending mode of the circle and the dominant role of the mode shown by Curve *a* in Figure 9). A residue-invariant decrease of Twist, which releases the excess Twist in the molecule, gradually comes into play (see Curve *c* in Figure 9 and the expressions in Table 3 for the variation of step parameters in the lowest frequency bending mode of the figure-8). The residue-invariant decrease of Twist becomes dominant when the configuration nears the intersection point in Figure 8, i.e., intermediate state, and further configurational rearrangement to the figure-8 proceeds almost exclusively through the release of excess Twist (noted by the color coding). Although the distribution of Twist along the contour of the intermediates is nonuniform, the incremental changes in overall twist, *Tw*, between successive configurational states is uniform, reflecting the regular increments of the writhe and the well-known invariance of the linking number ($Lk = Wr + Tw$).[46] The configurations adopted in the reverse transition from the figure-8 to the circle along Paths II and I′ are very similar to those shown in Figure 10. The energy barrier is slightly lower, ∼0.3 k_BT or ∼0.2 kcal/mol at 300 K, if the molecule follows Paths I and II′ from the circle to the figure-8, rather than the reverse Paths (II and I′) from the figure-8 to the circle, where the barrier is ∼0.5 k_BT or ∼0.3 kcal/mol at 300 K. It should be noted that explicit treatment of chain self-contact could change the normal-mode frequencies as well as the minimum energy of the figure-8 from the values computed here in the absence of such a correction.

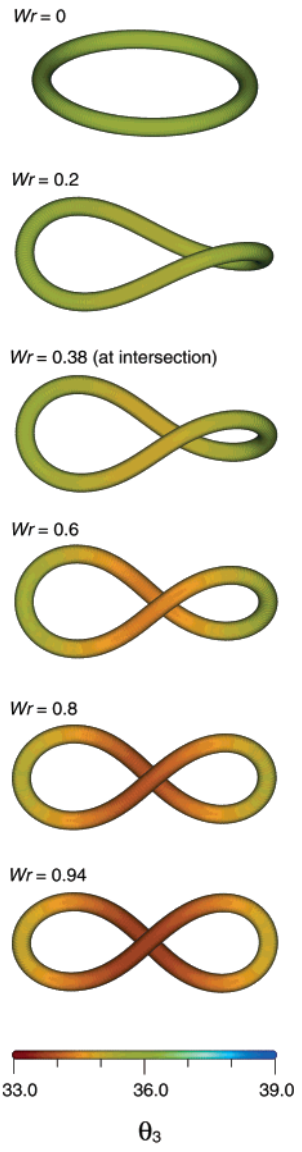

Figure 10. Computer-generated snapshots[52] of the configurational pathway between circular and figure-8 configurations obtained by deforming an overtwisted ($\theta_3^u = 34.25°$), naturally circular DNA minicircle along paths I and II′ in Figure 8. The color-coding of Twist is identical to that in Figure 4.

Discussion

The minicircles studied in this work are comparable in length and degree of supercoiling to the DNA loops which are formed by various regulatory proteins and enzymes that bind in tandem to sequentially distant parts of the long chain molecule.[47,48] The influence of natural curvature on the global motions of the minicircles found here can thus provide insight into how DNA loops of several hundred base pairs might respond to changes in nucleotide sequence. The sequence of base pairs in such loops determines the degree of intrinsic curvature of the spatially constrained molecule.[2−4]

Here we find that covalently closed DNA duplexes with natural curvature are torsionally stiffer but, when placed

under superhelical stress, are capable of greater bending deformations than minicircles which are made up of naturally straight DNA. The degree of curvature changes the character of global bending, i.e., the relative frequencies of in-plane vs out-of-plane deformations. Whereas a covalently closed, naturally straight duplex distorts more easily via in-plane than out-of-plane bending deformations, a natural minicircle is just as likely to bend via either route and a chain, which is curved more tightly than the natural minicircle, preferentially deforms out of the plane of the circle (Figure 3).

Whereas the naturally straight DNA rotates freely about its global helical axis, there is a barrier impeding large-scale helical twisting of curved DNA. In the absence of intrinsic curvature, no single orientation of the closed duplex is preferred over any other, and all sites are expected to be equally accessible to a ligand, such as DNase I, which preferentially contacts the (outer) convex surface of its DNA target.[49,50] By contrast, the introduction of natural curvature is predicted to restrict rotation of the DNA as a whole about its helical axis, thereby favoring the minimum energy configuration and limiting enzymatic access to residues located on the inside of the ring. The enzymatic cleavage pattern of a naturally closed DNA minicircle is thus expected to include regularly spaced sites of enhanced cutting alternating every half helical turn with sites of suppressed cutting. Other types of naturally closed molecules, such as curved DNA molecules generated from alternating fragments of naturally straight and naturally rolled base-pair steps,[14,15] are expected to exhibit the same global properties.

The barrier opposing global bending of the natural minicircle lowers significantly when the molecule is over- or undertwisted. The frequency, i.e., energy, of global bending decreases in value upon supercoiling (Figure 5), and if the imposed stress is sufficiently large, global configurational rearrangement of the circle to the figure-8 form takes place. Because the bending frequencies of the natural minicircle are much more sensitive to changes in intrinsic Twist than are those of the cyclized naturally straight polymer, the large-scale configurational interchange occurs more easily in the molecule with intrinsic curvature. The dominant ($n = 2$) modes of the two kinds of molecules, however, are of similar mixed bending character, i.e., the base pairs move out of the plane of the circle as the supercoiled molecule concomitantly deforms to elliptical shapes. The mechanism of conformational transformation between circle and figure-8 is thus expected to be similar in the two types of DNA.

Intermediate states constructed from the computed structures and dominant bending modes of the two minimum energy forms (Figures 8 and 10) suggest that the circle to figure-8 transformation involves two distinct types of conformational rearrangement. Localized changes in bending (Tilt and Roll) initially dominate as the circle deforms to an elongated, nonplanar intermediate state, and subsequent transformation to the figure-8 minimum proceeds via the uptake of twisting (Tables 2 and 3 and Figure 10). The twist density is nonuniform in both the intermediate states and the stable figure-8 minimum, with the imposed stress taken up preferentially at the sites of closest interstrand contact in the straighter central parts of the structures (Figure 4).

The range of low-energy states identified on the basis of the dominant normal modes of the circle and figure-8 is consistent with the mixture of spatial forms found in previous Monte Carlo simulations of a much longer (486 bp) DNA circle under superhelical stress.[51] The ($\sim$0.4 k_BT) potential barrier between the two states at the midpoint of the transition of the 200 bp natural minicircle is remarkably similar to the free energy (0.2 k_BT) reported previously for the longer, naturally straight DNA, with slightly different elastic constants and under the influence of a screened Coulombic potential. The present study tracks the lowest energy pathway of interconversion between circular and figure-8 configurations via the dominant thermal fluctuations of the two minimum energy states, whereas the Monte Carlo findings are based on the characteristics of a broad, random sample of configurational states. The treatment of normal modes provides mechanistic insights into configurational rearrangements which cannot be gleaned from Monte Carlo and other stochastic approaches.

Statistical mechanical considerations make it possible to characterize the large-scale motions in terms of the full set of normal-mode frequencies of covalently closed DNA molecules and can be applied to either computed or theoretically predicted modes (Figure 7). The thermal fluctuations in global structure are described in terms of the average deviation and variance of the writhe. The intrinsic, out-of-plane response of curved DNA to imposed torsional stress underlies its greater global deformability compared to a naturally straight molecule. The writhe, a measure of the chiral distortions from planarity of a closed curve, is sensitive to the intrinsic conformational response of curved DNA to imposed twist. The uniform twisting of base pairs along a curved, unligated molecule results in a helical configuration, the handedness and proportions of which depend respectively on the sign and magnitude of imposed twist. The same type of local deformations of an open piece of straight DNA merely reorients the bases at either end of the molecule without change of global shape. The covalent closure of the ends of the naturally curved duplex suppresses the torsionally induced configurational response of the linear molecule and converts the preferred helical configuration to the out-of-plane bending modes which dominate the global fluctuations of the closed polymer. The localized twisting of adjacent residues at a single site along a curved DNA similarly produces a chiral arc. The binding of an untwisting agent to a natural minicircle is therefore expected to enhance the global motions of a DNA minicircle by a similar mechanism, converting the end-to-end separation of the bound linear form into an out-of-plane bending mode in the closed molecule.

Finally, the remarkable agreement between the computed and theoretically predicted dependence of the normal modes of naturally curved DNA on the degree of curvature and torsional stress and the identical descriptions of the global motions of circular molecules add to the reliability of the normal-mode analysis of DNA at the base-pair level and increase confidence in the computed dynamic properties of

configurations such as the figure-8 which are beyond the scope of current theory.

Acknowledgment. Support of this work through U.S.P.H.S. Grant GM34809 and the New Jersey Commission on Science and Technology (Center for Biomolecular Applications of Nanoscale Structures) is gratefully acknowledged. Computations were carried out at the Rutgers University Center for Computational Chemistry.

Supporting Information Available: Animation files of the normal modes of a 200 bp DNA minicircle, which is naturally circular in its equilibrium rest state, governed by an ideal elastic potential, and subjected to torsional stress. This material is available free of charge via the Internet at http://pubs.acs.org.

References

(1) Olson, W. K.; Gorin, A. A.; Lu, X.-J.; Hock, L. M.; Zhurkin, V. B. DNA sequence-dependent deformability deduced from protein-DNA crystal complexes. *Proc. Natl. Acad. Sci., U.S.A.* **1998**, *95*, 11163−11168.

(2) Trifonov, E. N. DNA in profile. *Trends Biochem. Sci.* **1991**, *16*, 467−470.

(3) Crothers, D. M.; Drak, J.; Kahn, J. D.; Levene, S. D. DNA bending, flexibility, and helical repeat by cyclization kinetics. *Methods Enzymol.* **1992**, *212*, 3−29.

(4) Hagerman, P. J. Straightening out the bends in curved DNA. *Biochim. Biophys. Acta* **1992**, *1131*, 125−132.

(5) Laundon, C. H.; Griffith, J. D. Curved helix segments can uniquely orient the topology of supertwisted DNA. *Cell* **1988**, *52*, 545−549.

(6) Yang, Y.; Westcott, T. P.; Pedersen, S. C.; Tobias, I.; Olson, W. K. The effect of sequence-directed bending on DNA supercoiling. *Trends Biochem. Sci.* **1995**, *20*, 313−319.

(7) Chirico, G.; Langowski, J. Brownian dynamics simulations of supercoiled DNA with bent sequences. *Biophys. J.* **1996**, *71*, 955−971.

(8) Bauer, W. R.; Lund, R. A.; White, J. H. Twist and writhe of a DNA loop containing intrinsic bends. *Proc. Natl. Acad. Sci., U.S.A.* **1993**, *90*, 833−837.

(9) White, J. H.; Lund, R. A.; Bauer, W. R. Twist, writhe, and geometry of a DNA loop containing equally spaced coplanar bends. *Biopolymers* **1996**, *38*, 235−250.

(10) Charitat, T.; Fourcade, B. Metastability of a circular O-ring due to intrinsic curvature. *Eur. Phys. J. B* **1998**, *1*, 333−336.

(11) Olson, W. K. DNA higher-order structures. In *Oxford Handbook of Nucleic Acid Structure*; Neidle, S., Ed.; Oxford University Press: Oxford, U.K., 1999; pp 499−531.

(12) White, J. H.; Lund, R. A.; Bauer, W. R. Effect of salt-dependent stiffness on the conformation of a stressed DNA loop containing initially coplanar bends. *Biopolymers* **1999**, *49*, 605−619.

(13) Garrivier, D.; Fourcade, B. Twisting DNA with variable intrinsic curvature. *Europhys. Lett.* **2000**, *49*, 390−395.

(14) Coleman, B. D.; Olson, W. K.; Swigon, D. Theory of sequence-dependent DNA elasticity. *J. Chem. Phys.* **2003**, *118*, 7127−7140.

(15) Olson, W. K.; Swigon, D.; Coleman, B. D. Implications of the dependence of the elastic properties of DNA on nucleotide sequence. *Philos. Trans. R. Soc.* **2004**, *362*, 1403−1422.

(16) Zajac, E. E. Stability of two planar loop elasticas. *J. Appl. Mech. Trans. ASME Ser. E* **1962**, *29*, 136−142.

(17) Le Bret, M. Catastrophic variation of twist and writhing of circular DNAs with constraint? *Biopolymers* **1979**, *18*, 1709−1725.

(18) Benham, C. J. The onset of writhing in circular elastic polymers. *Phys. Rev. A* **1989**, *39*, 2582−2586.

(19) Young, M. A.; Srinivasan, J.; Goljer, I.; Kumar, S.; Beveridge, D. L.; Bolton, P. H. Structure determination and analysis of local bending in an A-tract DNA duplex: comparison of results from crystallography, nuclear magnetic resonance, and molecular dynamics simulation on d(CGCAAAAATGCG). *Methods Enzymol.* **1995**, *261*, 121−144.

(20) Sherer, E. C.; Harris, S. A.; Soliva, R.; Orozco, M.; Laughton, C. A. Molecular dynamics studies of DNA A-tract structure and flexibility. *J. Am. Chem. Soc.* **1999**, *121*, 5981−5991.

(21) Sprous, D.; Young, M. A.; Beveridge, D. L. Molecular dynamics studies of axis bending in $d(G_5\text{-}(GA_4T_4C)_2\text{-}C_5)$ and $d(G_5\text{-}(GT_4A_4C)_2C_5)$: effects of sequence polarity on DNA curvature. *J. Mol. Biol.* **1999**, *285*, 1623−1632.

(22) Strahs, D.; Schlick, T. A-tract bending: insights into experimental structures by computational models. *J. Mol. Biol.* **2000**, *301*, 643−663.

(23) McConnell, K. J.; Beveridge, D. L. Molecular dynamics simulations of B′-DNA: sequence effects on A-tract-induced bending and flexibility. *J. Mol. Biol.* **2001**, *314*, 23−40.

(24) Mazur, A. K.; Kamashev, D. E. Comparative bending dynamics in DNA with and without regularly repeated adenine tracts. *Phys. Rev. E* **2002**, *66*, art. no. 011917.

(25) Koehler, S. A.; Powers, T. R. Twirling elastica: kinks, viscous drag, and torsional stress. *Phys. Rev. Lett.* **2000**, *85*, 4827−4830.

(26) Scipioni, A.; Zuccheri, G.; Anselmi, C.; Bergia, A.; Samori, B.; DeSantis, P. Sequence-dependent DNA dynamics by scanning force microscopy time-resolved imaging. *Chem. Biol.* **2002**, *9*, 1315−1321.

(27) Porschke, D.; Schmidt, E. R.; Hankeln, T.; Nolte, G.; Antosiewicz, J. Structure and dynamics of curved DNA fragments in solution: evidence for slow modes of configurational transitions. *Biophys. Chem.* **1993**, *47*, 179−191.

(28) Chirico, G.; Collini, M.; Toth, K.; Brun, N.; Langowski, J. Rotational dynamics of curved DNA fragments studied by fluorescence polarization anisotropy. *Eur. Biophys. J.* **2001**, *29*, 597−606.

(29) Kremer, W.; Klenin, K.; Diekmann, S.; Langowski, J. DNA curvature influences the internal motions of supercoiled DNA. *EMBO J.* **1993**, *12*, 4407−4412.

(30) Klenin, K. V.; Frank-Kamenetskii, M. D.; Langowski, J. Modulation of intramolecular interactions in superhelical DNA by curved sequences. A Monte Carlo simulation study. *Biophys. J.* **1995**, *68*, 81−88.

(31) Katritch, V.; Vologodskii, A. The effect of intrinsic curvature on conformational properties of circular DNA. *Biophys. J.* **1997**, *72*, 1070−1079.

(32) Matsumoto, A.; Tobias, I.; Olson, W. K. Normal-mode analysis of circular DNA at the base-pair level. 1. Comparison of computed motions with the predicted behavior of an ideal elastic rod. **2005**, *1*, 117−129.

(33) Wang, J. C. Variation of the average rotation angle of the DNA helix and the superhelical turns of closed cyclic lambda DNA. *J. Mol. Biol.* **1969**, *43*, 25−39.

(34) Depew, R. E.; Wang, J. C. Conformational fluctuations of DNA helix. *Proc. Natl. Acad. Sci., U.S.A.* **1975**, *72*, 4275−4279.

(35) Anderson, P.; Bauer, W. Supercoiling in closed circular DNA: dependence upon ion type and concentration. *Biochemistry* **1978**, *17*, 594−600.

(36) Olson, W. K.; Marky, N. L.; Jernigan, R. L.; Zhurkin, V. B. Influence of fluctuations on DNA curvature. A comparison of flexible and static wedge models of intrinsically bent DNA. *J. Mol. Biol.* **1993**, *232*, 530−554.

(37) Tobias, I.; Olson, W. K. The effect of intrinsic curvature on supercoiling − predictions of elasticity theory. *Biopolymers* **1993**, *33*, 639−646.

(38) Dubochet, H.; Bednar, J.; Furrer, P.; Stasiak, A. Z.; Stasiak, A. Determination of the DNA helical repeat by cryo-electron microscopy. *Struct. Biol.* **1994**, *1*, 361−363.

(39) Tobias, I. Thermal fluctuations of small rings of intrinsically helical DNA treated like an elastic rod. *Philos. Trans. R. Soc.* **2004**, *362*, 1387−1402.

(40) Tobias, I.; Coleman, B. D.; Lembo, M. A class of exact dynamical solutions in the elastic rod model of DNA with implications for the theory of fluctuations in the torsional motion of plasmids. *J. Chem. Phys.* **1996**, *105*, 2517−2526.

(41) Tobias, I. A theory of thermal fluctuations in DNA miniplasmids. *Biophys. J.* **1998**, *74*, 2545−2553.

(42) Manning, R. S.; Hoffman, K. A. Stability of *n*-covered circles for elastic rods with constant planar intrinsic curvature. *J. Elasticity* **2001**, *62*, 1−23.

(43) Westcott, T. P.; Tobias, I.; Olson, W. K. Modeling self-contact forces in the elastic theory of DNA supercoiling. *J. Chem. Phys.* **1997**, *107*, 3967−3980.

(44) Miyashita, O.; Onuchic, J. N.; Wolynes, P. G. Nonlinear elasticity, proteinquakes, and the energy landscapes of functional transitions in proteins. *Proc. Natl. Acad. Sci. U.S.A.* **2003**, *100*, 12570−12575.

(45) Tomimoto, M.; Gō, N. Analytic theory of pseudorotation in five-membered rings. Cyclopentane, tetrahydrofuran, ribose, and deoxyribose. *J. Phys. Chem.* **1995**, *99*, 563−577.

(46) White, J. H. Self-linking and the Gauss integral in higher dimensions. *Am. J. Math.* **1969**, *91*, 693−728.

(47) Adhya, S. Multipartite genetic control elements: communication by DNA loop. *Annu. Rev. Genet.* **1989**, *23*, 227−250.

(48) Schleif, R. DNA looping. *Annu. Rev. Biochem.* **1992**, *61*, 199−223.

(49) Suck, D.; Oefner, C. Structure of DNase I at 2.0 Å resolution suggests a mechanism for binding to and cutting DNA. *Nature* **1986**, *321*, 620−625.

(50) Lahm, A.; Suck, D. DNase I-induced DNA conformation. 2 Å structure of a DNase I-octamer complex. *J. Mol. Biol.* **1991**, *221*, 645−667.

(51) Gebe, J. A.; Schurr, J. M. Thermodynamics of the first transition in writhe of a small circular DNA by Monte Carlo simulation. *Biopolymers* **1995**, *38*, 493−503.

(52) Kraulis, P. J. MolScript: a program to produce both detailed and schematic plots of protein structures. *J. Appl. Crystallogr.* **1991**, *24*, 946−950.

CT049949S